Robust Map Registration for Building Online Glass Confidence Maps

Jun Jiang * **Renato Miyagusuku** ** **Atsushi Yamashita** *
Hajime Asama *

* *Department of Precision Engineering, Graduate School of Engineering, The University of Tokyo, Japan (email: {jiang, yamashita, asama}@robot.t.u-tokyo.ac.jp)*
** *Department of Mechanical and Intelligent Engineering, Graduate School of Engineering, Utsunomiya University, Japan (email: miyagusuku@ir.utsunomiya-u.ac.jp)*

Abstract: Laser rangefinders (LRFs) are widely used in mobile robot localization. However, glass, which is common in indoor environments, can only be detected by LRFs in limited incident angles, instead of all incident angles like other objects. As common representations of the environments do not consider this property, glass can negatively influence the robot's localization accuracy by causing a mismatch between measurements and the map even when locations are correct. A solution to this problem is to build a glass confidence map, which shows the probability of each object in the environment to be glass. If glass confidence maps want to be built online, it is important to consider pose uncertainty. Pose uncertainty can cause incorrect registration of glass probabilities, i.e., the incorrect grid is assigned the computed glass probability. In this work, we propose a robust registration method that explicitly considers pose uncertainty. The proposed method is verified experimentally, and results show that glass confidence maps can be built online successfully and with high accuracy.

1. INTRODUCTION

Localization is fundamental for mobile robots to perform other various tasks, such as search and rescue, housework and elderly care. Besides, there is a high potential for the use of mobile robots in indoor human environments, such as homes, shopping malls, and offices, where glass is common, as shown in Fig. 1. Therefore, being able to localize accurately and robustly in glass environments is important for mobile robots.

Techniques like Simultaneous Localization and Mapping (SLAM) have been developed in order to enable robots to localize automatically and online. Several current SLAM algorithms use Laser rangefinders (LRFs), because of their high accuracy for measuring distances. However, LRF-based SLAM systems perform unsatisfactorily in glass environments because glass can only be detected by LRFs in limited angles, instead of in any angles for other objects (Foster et al., 2013). This limitation disturbs the existing scan matching schemes (Moon et al., 2010), and consequently negatively influences localization accuracy.

Previous research dealt with the above-mentioned localization and mapping problems in glass environments. To improve localization accuracy, Munoz and Pimentel (2005) changed localization error function to give less penalty to large distance mismatch caused by glass. However, experiment results showed their method only worked well when the glass area is small. Additionally, Kim and Chung (2016) built a localization method which analyzed all possible situations caused by up to two layers of glass. Experimental results showed their method improved the robot's localization accuracy greatly at the cost of much higher computational cost, as all possible situations are considered. Koch and Nchter (2017) and Koch et al. (2017) enhanced current SLAM systems by first classifying LRF scan points into several types, such "transpent surface" or "behind transpent", and discarding certain error-prone

Fig. 1. Glass is very common in human indoor environments (Jiang et al., 2017).

types of points while building maps. However their method classified LRF scan points seperately every time they are received, and did not take advantages that the same object would be scanned for multiple times while robot is moving. This caused their results less relaible, and in their work, further pose process is recommended.

We previously proposed to build a glass confidence map aiming to improve the localization accuracy in glass environments (Jiang et al., 2017). The glass confidence map shows objects' probabilities of being glass on the map, which can be used to, for example, adjust the penalty of error caused by glass, or reduce the computational burden of Kim and Chung (2016). In order to build glass confidence maps, our previous work proposed the use of a neural network-based classifier. The network computes a pseudo-probability of objects to be glass or non-glass. Pseudo-probabilities were updated using incoming measurements as well as the occupancy grid map (Elfes, 1989) of the environment, which could only be obtained after all measurements were acquired. Therefore, in a new environment whose occupancy grid map is unknown, it would be necessary to run a SLAM algorithm first in order to build the occupancy grid map, and then build the glass confidence map in post-processing. This limits the potential use of the glass confidence map for improving the localization component of SLAM approaches. If our previous approach is applied directly after each partial map is generated by the SLAM algorithm, pose uncertainty causes incorrect registration of glass probabilities, i.e., the incorrect grid in the occupancy map is assigned the computed glass probability. In this paper, we focus on robust glass probability registration aimed to enable glass confidence maps to build online, robustly and with high accuracy.

The rest of this paper is organized as follows: Section II provides an overview of the previously proposed neural network classifier and the offline glass probability registering method, for a better understanding of this work. Section III introduces the newly proposed online glass probability registering method, and also the combination of it with the neural network glass classifier described in Section II. Section IV presents verification experiments in an office-like building. Finally, conclusions and future works are drawn in Section V.

2. OVERVIEW OF GLASS CLASSIFIER

The main physical principle governing LRFs is light reflection. LRFs work by sending a laser beam of light and waiting for its return once it has hit the nearest object in its path. By measuring the time of flight required by the laser beams to return, LRFs can very accurately calculate the distance to the object that caused the reflection. Other than the distance to the closest object, LRFs also provide the energy of the received laser beam. Received energy depends on the distance to the object, the transparency and reflective index of the object, and the incident angle at which the laser beam hits the object.

As glass and non-glass objects have very different transparency and reflective indexes, it is possible to classify objects like glass or non-glass based solely on their LRF intensities when taking into consideration the influence of distance and incident angle. Using this idea, in our previous work we proposed a glass classifier using a neural network. The proposed network considered the distance d and received intensity i measured by the LRF, as well as the incident angle θ of the laser beam with respect to the object. The system worked by having the robot use its equipped LRF to continuously scan the environment, emitting n laser beams evenly distributed in its scanning angle range, and collecting the reflected beams. Using this information, the sensor calculates distances based on time of flight and outputs both the distances as well as the received intensities for each of the n beams. Distances are then used to compute the incident angles of the laser beams by detecting straight lines using Hough Transform (Ballard, 1981).

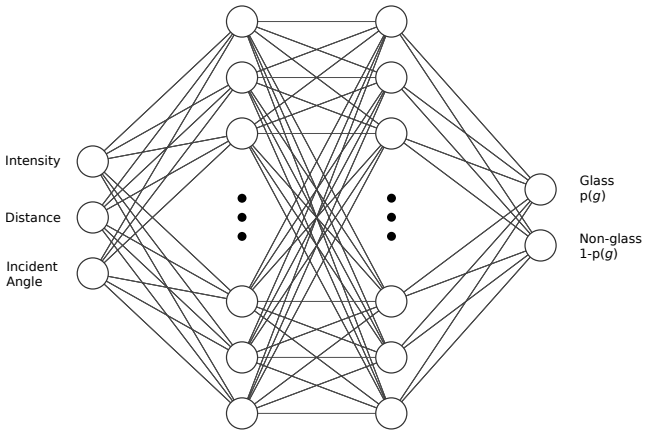

Fig. 2. Structure of the neural network employed in our previous work (Jiang et al., 2017).

Using extensive labeled training data, the glass classifier learns how to detected if an object is glass or non-glass. That is, it learns the mapping

$$f(i, d, \theta) \rightarrow g \tag{1}$$

with g being the objective class.

Specifically, the employed network was a simple 4-layer fully connected neural network, as the one shown in Fig. 2, with a softmax function on the output layer. The softmax function was used so the outputs of the network would be pseudo-probabilities p(g) (for training values larger than 0.5 were considered glass, and otherwise non-glass)

Using this network, for all n beams the vector $\mathbf{p_g} = \{f(i_k, d_k, \theta_k)\}_{k=1}^{n}$ could be computed. Experimental validations showed that this network was indeed capable of correctly classifying glass and non-glass objects.

3. ONLINE GLASS CONFIDENCE MAP BUILDING

3.1 System Overview

The outline of our approach for building online glass confidence maps is shown in Fig. 3, with the component newly proposed in this paper being the improved glass probability registering method, marked in red.

Our proposed system records both distances to objects as well as received signal intensities from a single LRF. Using the same incident angle calculator and neural network glass classifier used in our previous work, glass probabilities $\mathbf{p_g}$ are calculated using distance information for

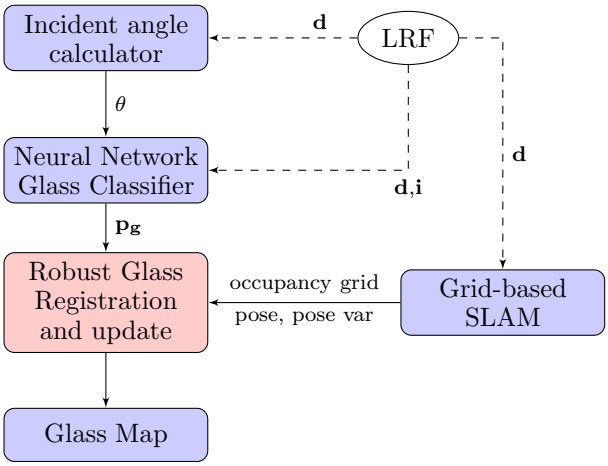

Fig. 3. Overview of the proposed online glass confidence mapping system. In this work we focus on the Robust Glass Registration and Update module

each scan. As the robot moves through the environment, a grid-based SLAM algorithm estimates robot pose and its uncertainty and updates an occupancy grid map of the environment. While any grid-based SLAM approach can be used, for our testing we employed the one described in Grisetti et al. (2005). Using robot pose, pose uncertainty, grids' occupancy, and glass probability information, our proposed registration algorithm registers, and updates glass probabilities onto a temporary glass map. This temporary glass map explicitly considers pose uncertainty when updating glass probabilities, enabling a more robust registration. Nonetheless, it can not filter outliers and may not match the latest occupancy map. In order to remove noise and be congruent with the latest occupancy probabilities, the temporary map is filtered in order to obtain the glass confidence map. As described before, the obtained glass confidence map can be used with SLAM to improve robot's localization accuracy, which will be considered in future work.

3.2 Robust Registration

Once glass probabilities have been computed, it is necessary to update the glass probabilities of their corresponding cells in the grid map. We refer to this problem as probability registration. Formally, we need to compute which grid map cell c or set of cells C that should be updated using the glass probability $\mathrm{p}(g_j)$ computed from the LRF's jth laser scan. To compute this we make the following assumptions:

(i) Robot's pose ($\boldsymbol{x}$) has a Gaussian distribution with variance σ_x^2, i.e., $\boldsymbol{x} \sim \mathcal{N}(\hat{\boldsymbol{x}}, \sigma_x^2)$.
(ii) Distance measurement ($\boldsymbol{l}_j$), in map coordinates, also has Gaussian distribution with variance σ_l^2, i.e., $\boldsymbol{l}_j \sim \mathcal{N}(\hat{\boldsymbol{l}}_j, \sigma_l^2)$.
(iii) As LRFs distance measurements are considerably more precise than robot pose estimates its covariance is considered much lower than that of robot poses, i.e., $\sigma_l^2 << \sigma_x^2$.
(iv) Robot's pose and distance measurements are independent random variables.

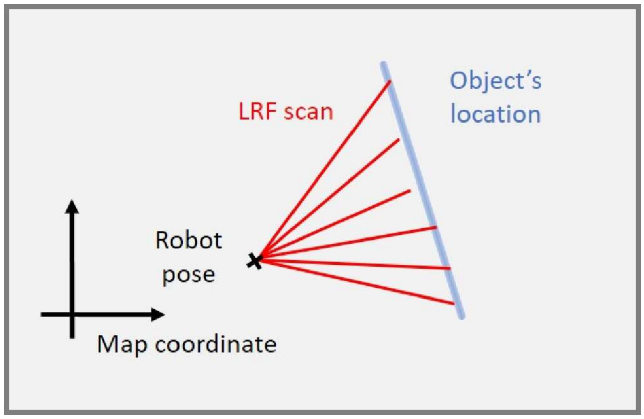

(a) If no uncertainty exists in robot pose or LRF measurements, the wall's location can be fully determined.

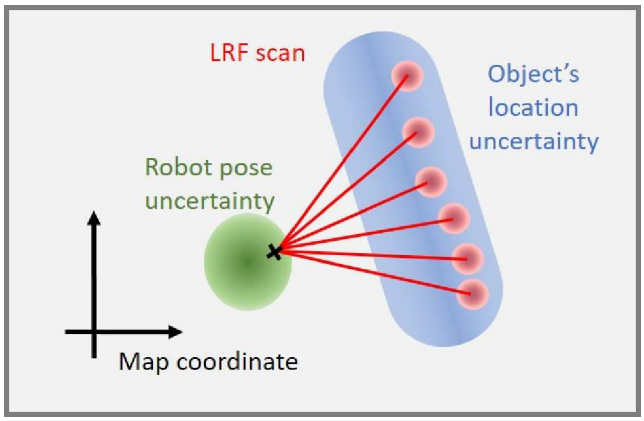

(b) When considering robot pose and LRF measurements uncertainties, the wall' location should be represented by a probabilistic distribution.

Fig. 4. Illustration of probabilistic distributions of robot pose, LRF measurements and measured wall locations (in green, red and blue respectively). Darker shades represent higher probabilities.

Given these considerations, we can approximate $\sigma_x^2 + \sigma_l^2$ to σ_x^2 and hence the distribution of the end point of scan j becomes

$$\boldsymbol{x}_j = \mathcal{N}(\hat{\boldsymbol{x}} + \hat{\boldsymbol{l}}_j, \sigma_x^2). \tag{2}$$

For any cell c in the grid map with coordinates $\mathbf{c}$, the likelihood of the cell to be the true location $\boldsymbol{x}_j$ is then calculated as

$$\mathrm{p}(c = \boldsymbol{x}_j) = \frac{1}{\sigma_x} \varphi\left(\frac{|\boldsymbol{x} - \mathbf{c}|}{\sigma_x}\right), \tag{3}$$

where $\varphi(x) = \frac{1}{\sqrt{2\pi}} \exp\left(-\frac{1}{2}x^2\right)$ is the standard normal distribution.

For map registration, we analyze two scenarios: 1) low robot pose uncertainty, and 2) arbitrary robot pose uncertainty. Figure 4 illustrates both cases. In Fig. 4 (a), we can observe that under low pose uncertainty, the likelihood of any grid cell to be the true location $\boldsymbol{x}_j$, other than the nearest occupied cell $\hat{c}_j$, is low. On the contrary, if a relatively larger pose uncertainty is considered, as in Fig. 4 (b), several grid cells have similar likelihoods.

Low pose uncertainty In our previous approach, for any scan j only the nearest occupied cell $\hat{c}_j$ was updated. This

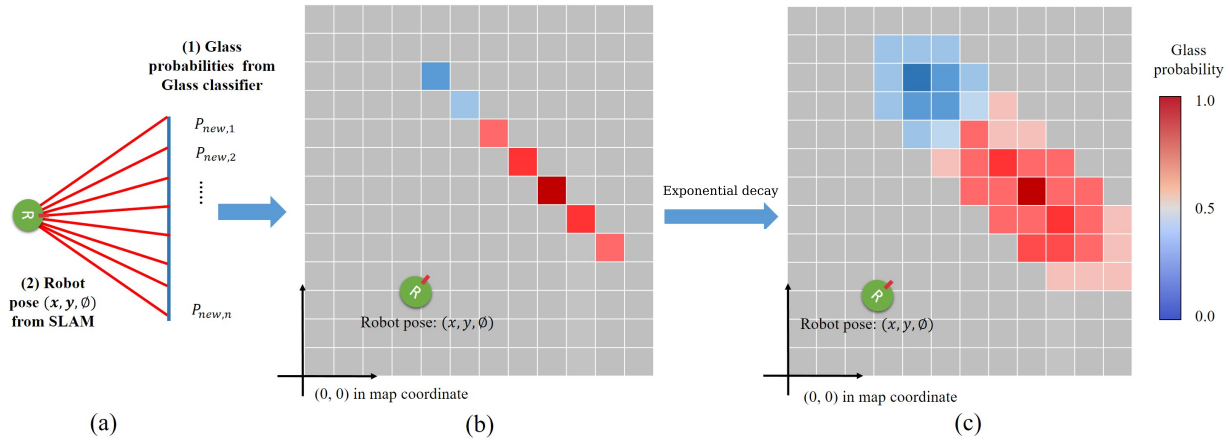

Fig. 5. Process of registering and updating the glass probability onto a temporary glass map.

registration method can be derived if pose uncertainty is assumed to be considerably low.

By definition, the distance between $\hat{\boldsymbol{x}}_j$ and $\hat{c}_j$ is the lowest among all occupied cells. Then, the distance between the location of any occupied cell $\mathbf{c}$ and $\hat{\boldsymbol{x}}$ can be expressed in terms of two non-negative values e and δ, with e being $|\boldsymbol{x} - \hat{c}|$, and $e + \delta = |\boldsymbol{x} - \mathbf{c}|$. Equation (3) can then be re-written as

$$\mathrm{p}(c = \boldsymbol{x}_j) = \frac{1}{\sigma_x}\varphi\left(\frac{e+\delta}{\sigma_x}\right) \tag{4}$$

$$= \mathrm{p}(\hat{c}_j = \boldsymbol{x}_j)\exp\left(-\frac{1}{2}\frac{\delta^2}{\sigma_x^2}\right). \tag{5}$$

For values of δ twice of σ_x we the likelihood of cell c drops to 0.13% and for δ values 3 times of σ_x it drops to around 1%. Under this low pose uncertainty assumption, the right hand exponential term makes $\mathrm{p}(c = \boldsymbol{x}_j)$ become considerably lower even for cells c adjacent to $\hat{c}$. This assumption is fair for offline SLAM approaches whose resulting occupancy grid maps have been updated with all measurements acquired along the whole robot's trajectory and whose pose uncertainties have been minimized. However, when performing online mapping, this assumption does not hold, as robot pose uncertainties are often comparable if not larger than grid map resolutions of typically 5 cm.

Arbitrary pose uncertainty Our current approach can be considered an extension of the previous one, where we relax the low pose uncertainty assumption. If we are to register glass probabilities to multiple grid cells two options are viable. Either update the probability of all *likely* grids using $\mathrm{p}(g_j)$, where the definition of likely needs to be addressed, e.g., within two standard deviations. Or, update grid probabilities taking into consideration the likelihood of the grid to be the true location of the endpoint $\boldsymbol{x}_j$. In this work, we opted for the second option, and propose a method to register glass probabilities to multiple cells with varying degrees of confidence.

Therefore, the problem now becomes how to modify $\mathrm{p}(g_j)$ as to reflect this varying confidence. An alternative is to assume $\mathrm{p}(g_j)$ has been generated from a known probability distribution, and then increase the distribution's concentration parameter according to the likelihood $p(c = \boldsymbol{x}_j)$. For example, for a Gaussian distribution, we would increase its variance for less likely cells. The issue we encounter with such an approach is that outputs from the neural network glass classifier do not belong to any particular probability distribution family, what is more, it does not even have a proper probability distribution but rather a pseudo-probability obtained by normalizing $\mathrm{p}(g_j)$ and $\mathrm{p}(\neg g_j)$ to sum up to 1.

Instead of assuming a particular distribution for $\mathrm{p}(g_j)$, we use an exponential decay equal to the right hand term of eq. (5) to reduce its certainty. Specifically, we compute the glass probability at cell c, $p(g_j, c)$, as

$$\mathrm{p}(g_j, c) = (\mathrm{p}(g_j) - 0.5)\exp\left(-\frac{1}{2}\frac{|\boldsymbol{x}_j - \mathbf{c}|^2}{\sigma_x^2}\right) + 0.5. \tag{6}$$

This equation results from assigning the probability generated by the neural network classifier to the nearest neighbor $\hat{c}_j$, $\mathrm{p}(g_j, \hat{c}) = p(g_j)$, and penalizing neighboring cells using the aforementioned exponential decay. We formulate this equation so that when $\delta \to \infty$, $p(g_j, c)$ tends to 0.5, as this is the uninformative probability. A glass probability lower than 0.5, implies that observed cell is not glass.

3.3 Probability Update

Regardless of the registration method of choice, the following equation is used to update its glass probability if it already has a prior probability registered to it

$$p_{post} = \frac{p_{prior}\mathrm{p}(g_j, c)}{p_{prior}\mathrm{p}(g_j, c) + (1 - p_{prior})(1 - \mathrm{p}(g_j, c))}, \tag{7}$$

where p_{prior} is the grid's previous glass probability, and p_{post} is its glass probability after incorporating $\mathrm{p}(g_j)$. The updated probability p_{post} serves as new p_{prior} if another glass probability needs to be incorporated.

This equation is derived under the assumption that each new $\mathrm{p}(g_j, c)$ is independent of each other. An uninformative prior $p_{prior} = 0.5$ is assumed when no measurements have been obtained for any particular cell.

3.4 Implementation considerations

Figure 5 shows our registration and update process. For each LRF scan, corresponding glass probability $\mathrm{p}(g_j)$

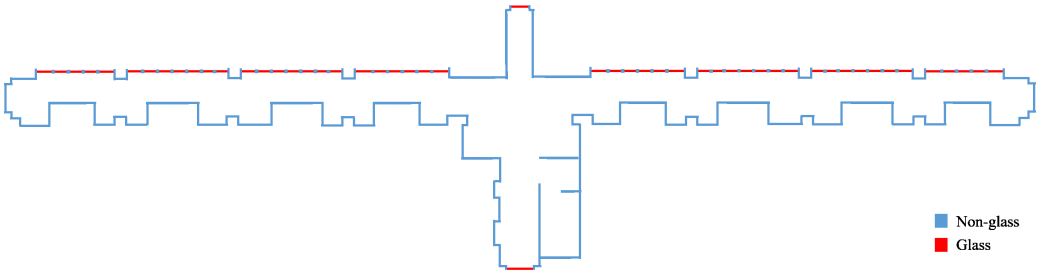

(a) Blueprint of the experimental environment (ground truth)

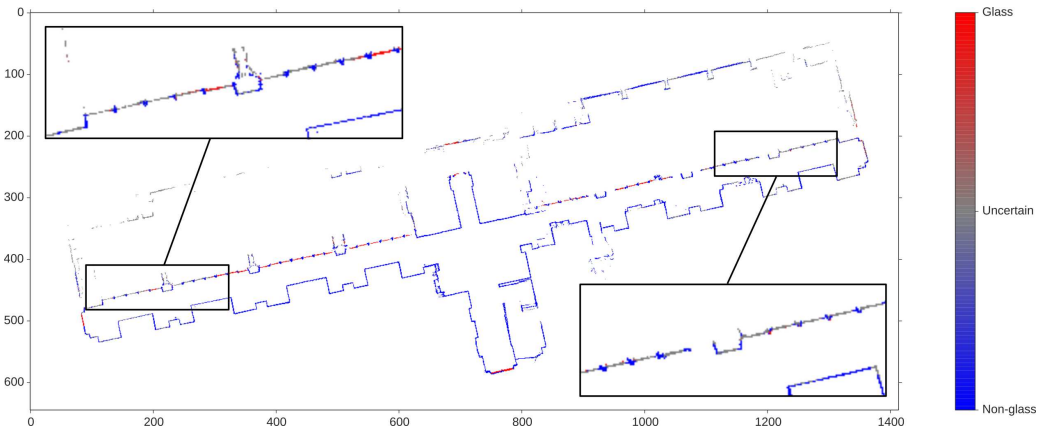

(b) Test 1: The map changing problem causes a lot of occupied grids are in gray, meaning not enough glass probability were registered correctly for them

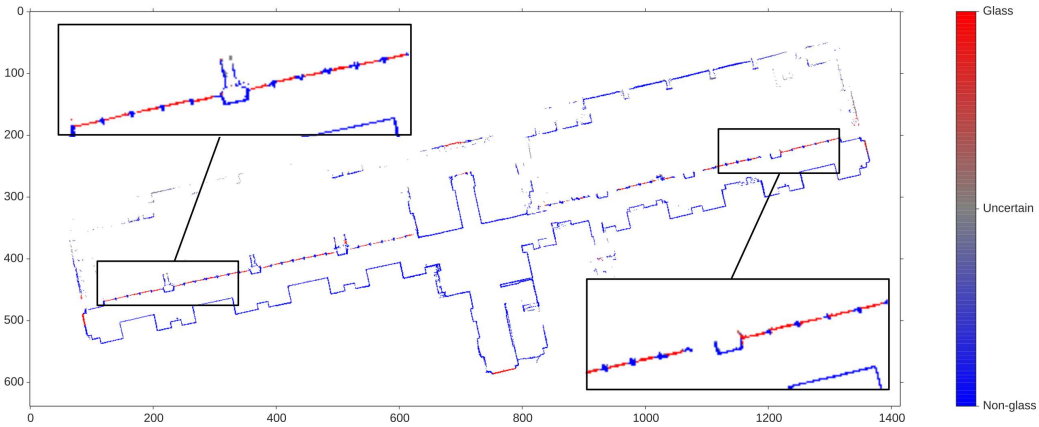

(c) Test 2: Most grids are registered correctly as glass or non-glass, which shows the advantages of our robust registration method

Fig. 6. Generated glass confidence maps with different registration methods

and nearest occupied cell $\hat{c}$ are computed. To reduce computational cost, $\mathrm{p}(g_j, c)$ is computed only for grids c close to $\hat{c}$, specifically either the 3×3 or a 5×5 grids around $\hat{c}$. Using eq. (7) the probabilities in these grids are then updated onto a temporal map.

Whenever a glass map is requested, our system inspects only the cells in its temporal glass map which correspond to occupied cells in the latest occupancy grid map available. These grids are then overlain over the occupancy grid map, showing glass probabilities in different shades of red for glass and blue for non-glass. This additional filtering step serves to match glass and occupancy maps as well as to reduce noise and outliers.

4. EXPERIMENT VERIFICATION

To validate the proposed method, experiments were performed in an indoor environment.

4.1 Environment and Settings

The testing environment is shown in Fig. 1, an office-like environment where a large area of glass exists. For evaluation, the blueprint of the environment that shows glass and non-glass objects, Fig. 6(a), was used as the ground truth. Please note that LRF may see wall/objects behind glass and show them on the map. However, in this environments, the wall behind glass is outdoors and partly invisible to LRF due to strong sunlight outsides. Therefore,

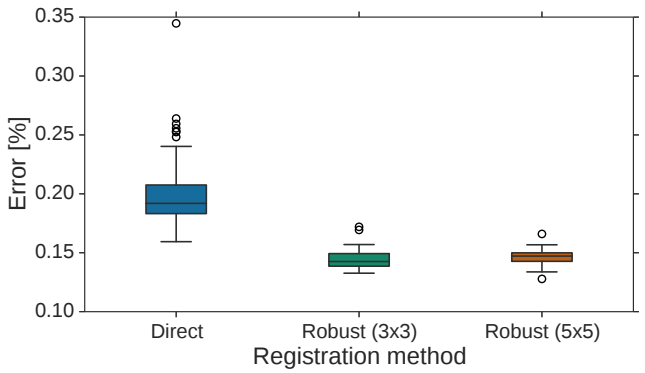

Fig. 7. Percentage of classification errors: direct registration, and robust registration with 3x3 and 5x5 grids

they are exculded from evaluation and is not shown on ground truth. The experiment was performed using a Pioneer 3-DX mobile robot, a Hokuyo UTM 30LX-EW LRF mounted in the front of the robot, and a ThinkPad P50 laptop to process data and build the map. Our system ran on Ubuntu 16.06 and the Robot Operating System (ROS) Kinetic version, with gmapping (Grisetti et al., 2005) was used to implement SLAM and generate the occupancy grid map required by our method.

4.2 Results and Discussions

Glass probability maps were build using either the low pose uncertainty assumption (direct registration), where only the nearest occupied cell was updated, or our proposed robust registration method (considering either 3×3 or 5×5 grids). Due to the probabilistic nature of the SLAM algorithm used, using the data collected in our testing environment, 50 tests were performed.

Figures 6(b) and 6(c) show examples of the glass confidence maps obtained with direct and robust registration respectively. In these maps, unoccupied areas are shown in white, while unknown areas are shown in green color. For the occupied areas, glass probabilities are shown in different colors, changing from blue (100% certain of being non-glass) to red (100% certain of being glass); gray shows high uncertainty, which usually because too little glass probability is registered to these grids. In each map, the same area is enlarged for better observation. Figure 7 shows the percentage of classification errors obtained for each registration method. Percentages were computed considering only the areas of the map that have both walls and glass, as these are our areas of interest.

From Fig. 6(c) we can observe that our proposed method can successfully build glass confidence maps online. Figure 7 shows that our robust registration method not only has lower mean classification errors but also considerably lower worst performance, as well as more consistent results (lower variance). Therefore, it can be argued that it is more robust. Finally, as experimental results show that using either 3x3 or 5x5 grids give similar results, 3x3 grids are recommended due to their lower computational demands on the system.

5. CONCLUSIONS AND FUTURE WORK

In this paper, to enable robust online glass confidence mapping, a new glass probability registration method was proposed. In the proposed method, glass probabilities are registered online based on robot pose and LRF measurements, without needing a completed occupancy grid map of the environment. An experiment was performed in an office environment, in order to verify the proposed method. Results show that the proposed method consistently generates more accurate glass probability maps than the previous approach utilized. Future works related to this paper are mainly about using the built glass confidence map to improve the robot's localization in glass environments.

ACKNOWLEDGMENT

This work was partly funded by The Okawa Foundation for Information and Telecommunications.

REFERENCES

Ballard, D.H. (1981). Generalizing the hough transform to detect arbitrary shapes. *Pattern Recognition*, 13(2), 111–122.

Elfes, A. (1989). Using occupancy grids for mobile robot perception and navigation. *Computer*, (6), 46–57.

Foster, P., Sun, Z., Park, J.J., and Kuipers, B. (2013). VisAGGE: Visible angle grid for glass environments. In *Proceedings of the 2013 IEEE International Conference on Robotics and Automation (ICRA 2013)*, 2213–2220.

Grisetti, G., Stachniss, C., and Burgard, W. (2005). Improving grid-based slam with rao-blackwellized particle filters by adaptive proposals and selective resampling. In *Proceedings of the 2005 IEEE International Conference on Robotics and Automation (ICRA 2005)*, 2432–2437.

Jiang, J., Miyagusuku, R., Yamashita, A., and Asama, H. (2017). Glass confidence maps building based on neural networks using laser range-finders for mobile robots. In *Proceedings of 2017 IEEE/SICE International Symposium on System Integration (SII 2017)*, 405–410.

Kim, J. and Chung, W. (2016). Localization of a mobile robot using a laser range finder in a glass-walled environment. *IEEE Transactions on Industrial Electronics*, 63(6), 3616–3627.

Koch, R., May, S., Murmann, P., and Nüchter, A. (2017). Identification of transparent and specular reflective material in laser scans to discriminate affected measurements for faultless robotic slam. *Robotics and Autonomous Systems*, 87, 296–312.

Koch, Rainer, S.M. and Nchter, A. (2017). Effective distinction of transparent and specular reflective objects in point clouds of a multi-echo laser scanner. In *Proceedings of 2017 IEEE International Conference on Advanced Robotics (ICAR 2017)*, 566–571.

Moon, C., Chung, W., and Doh, N.L. (2010). Observation likelihood model design and failure recovery scheme toward reliable localization of mobile robots. *International Journal of Advanced Robotic Systems*, 7(4), 113–122.

Munoz, L.R. and Pimentel, J.J.A. (2005). Robust local localization of a mobile robot using a 180/spl deg/2-d laser range finder. In *Proceedings of the Sixth Mexican International Conference on Computer Science (ENC 2005)*, 248–255.